The Role of Ultrasonic Anemometry in Wind Energy

A. Martinez, A. Cuerva, A. Sanz-Andrés , S. Franchini.
Instituto Universitario de Microgravedad "Ignacio Da Riva" (IDR/UPM), E.T.S.I. Aeronáuticos, Universidad Politécnica de Madrid, 28040 Madrid-Spain
Tel. 00 34 91 336 63 53. Fax. 00 34 91 336 63 63. alejandro.martinez@upm.es

1. Introduction.

Most of the experimental tasks in Wind Energy require the determination of the 3D turbulent characteristics of the wind speed with large time resolution. Ultrasonic anemometers are able to provide measurements of the wind speed vector in one point with time resolutions ranging from 1 up to 100 samples per second. Additionally they are robust, and only need one initial calibration. These requirements are generally not fulfilled by cup anemometers.

However not all the problems regarding sonic anemometers are solved. Their response is highly dependent on the geometry and operational parameters of the sensor. Additionally vibration of the measuring system can affect the measurement. Measured spectra and derived parameters such as turbulence intensities, friction velocities or length scales of the flow, all of them very important in Wind Engineering, can contain important errors if the proper correction methods are not applied.

This paper shows the state of the art in the modelling of sonic anemometers measuring process. These models are useful to optimize the design of sonic anemometers or to obtain correction functions for the measured spectra. The response of the sonic is modelled considering the following input parameters: the geometry of the sensor, the operational characteristics (sampling rate), the mean wind direction and vertical inclination and the averaged Mach number of the flow.

Additionally, latest techniques for wind tunnel calibration of sonic anemometers are presented focusing on automatic calibration sequences oriented to reduce the wind tunnel operation time needed for calibration. Part of the results delivered in the ACCUWIND project by IDR-UPM, DEW and RISØ are presented [1].

Finally an insight on the recent developments on rotating sonic anemometers intended to be installed of wind turbine hubs is presented.

2. Modelling of ultrasonic anemometers.

A Sonic anemometers is an intrusive and averaging sensor, therefore it affects the mesurand be it the real wind speed, or other flux parameters, such as real virtual temperature or friction velocity. First a line averaging effect exists, which means that each sonic measurement is an average of the real values along measuring paths [28]. Also the averaged values are not done on the real magnitudes since the flow is disturbed by the presence of the sensor in two ways: first upwind (blocking effect) and second by wakes generated by transducers and supporting structures [17]. An example of the distortion of the measurement provoked by the transducer heads is shown in Figure 4 for a single path. Also temperature and deposits may affect the measurements [15].

The distortions of the measurements can be solved at least in two ways: a) by modifying the design or b) by correcting the measured data. The first option is always better, when possible.

The above mentioned factors affects the capacity to measure averaged values and turbulent magnitudes of the wind speed vector, making necessary a proper calibration process in wind tunnel.

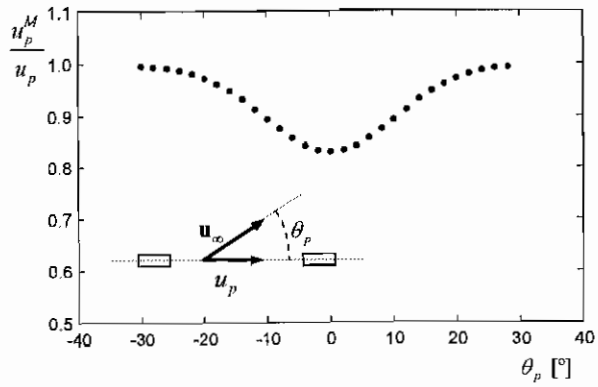

Fig. 4. Fig. 1. Transducer shadow effect represented as the ratio of the measured wind speed along the path and the real wind speed along the path up as a function of the angle θ_p formed by the path and the wind speed vector predicted by the Windgaard model [41]. The case presented corresponds to a ratio $l/d = 20$, l and d being the length of the acoustic path and the characteristic diameter of the transducer head respectively.

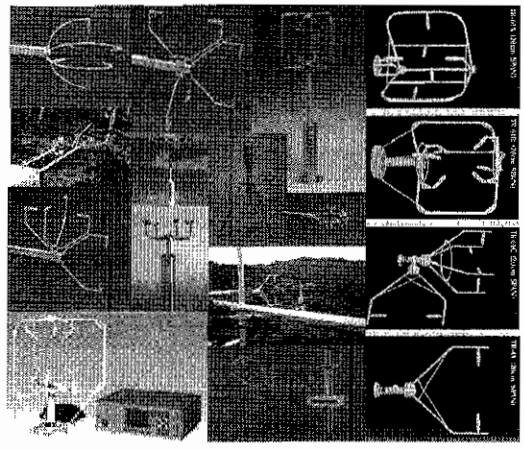

Fig. 5. Fig. 2.Different models of sonic anemometers.

Although some standard information exists [1], [2], [38], calibration in wind tunnel is one of the most challenging tasks regarding sonic anemometers since this type of sensor require a time intensive calibration process. Theoretically, the calibration process consists in determining the relation of three components of the wind speed vector **u** measured by a reference sensor in a wind tunnel and the three components of the vector measured by the SA. This process requires the determination of a function defined $\mathbf{f}_c$: $R^3 \rightarrow R^3$ which means a complexity two orders of magnitude larger than in the cup anemometer case. It is expected that the highest sensitivity of function $\mathbf{f}_c$ is respect to azimuthal variations of wind incidence, although it can be evidenced that it is also sensitive to variations of the wind speed inclination angles and to variations in the module of the wind speed vector. A priori the shape of function $\mathbf{f}_c$ must be determined in a full range test where a complete interval of wind speed module u, wind speed azimuth angle θ and wind speed azimuth inclination angle γ are covered.

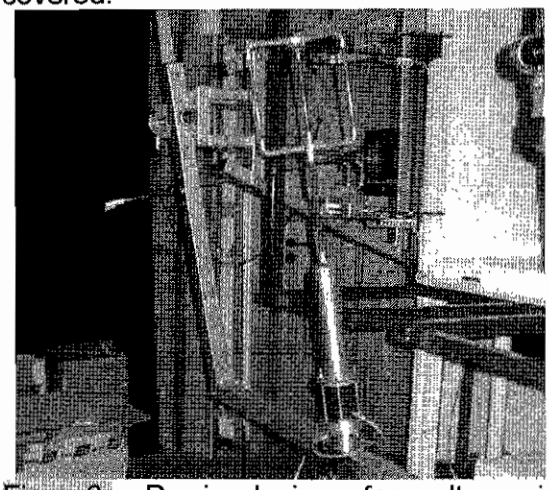

Fig. 3. Dewi device for ultrasonic calibration.

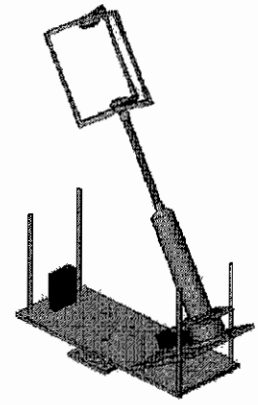

Fig. 4. IDR device for ultrasonic calibration.

From this approach two main problems arise, first the need to reduce the calibration time, deciding in a smart way which is the number of discrete values of **u**, θ and γ at which the anemometer must be calibrated in order to obtain an accurate enough calibration function $\mathbf{f}_c$, and second, how to manage and present

the calibration results is an practical and traceable way for accreditation purposes.

Considering the first point, some adaptative algorithms are tested within the ACCUWIND project, trying to minimize the calibration time within a certain degree of accuracy.

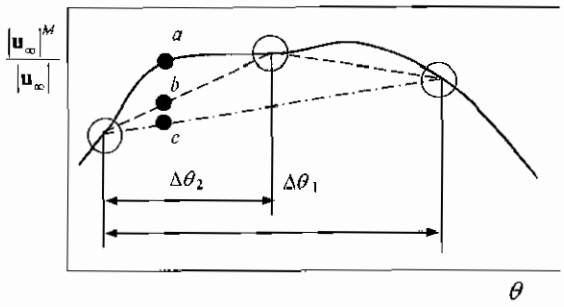

Fig 9: Fig. 5. Scheme of the process of automatic determination of test points in a single variable test (θ). It is represented the ratio of measured wind speed module on the real value versus the angle on incidence of the wind speed vector θ obtained in a calibration test for horizontal wind speed in wind tunnel. The dots represent the experimental values, the continuous line represent the ideal calibration curve (Very large azimuthal resolution) whereas the dotted-dashed and dashed lines represent the calibration curves for to real cases with azimuthal resolution $\Delta\theta_1$ and $\Delta\theta_2$ respectively. The segment *a-b* represents the maximum calibration error in the calibration curve based in $\Delta\theta_2$ is used whereas the segment *a-c* represents the maximum calibration error in the calibration curve based in $\Delta\theta_1$ is used.

Therefore, after defining certain error parameter, that can be an average or maximum error between the calibrated and real response (i.e maximum allowed error in the determination of the wind speed module) the values of **u**, θ and γ to be tested are automatically chosen to comply with the restriction.

In Figure 9 a scheme of two calibration curves for an horizontal wind speed case are presented. In one case the ratio between measured and real wind speed module is determined experimentally each $\Delta\theta_1$ angle of wind incidence, whereas in the second case a value is obtained each $\Delta\theta_2=\Delta\theta_1/2$. As can be observed the maximum calibration error (measured respect to an ideal calibration function) is reduced from *a-c* down to *a-b*. If a maximum allowed calibration error ε_C is decided, the azimuthal step $\Delta\theta$ is reduced down up to reach such allowed value. This is done for different azimuthal sectors so that those directions with larger variations in ratio between measured and real wind speed magnitudes are automatically assigned a lesser value of $\Delta\theta$.

Regarding the second problem, the presentation of results, it is remarked that the calibration of a sonic anemometer might involve the determination of the function $\mathbf{f}_c$: $R^3 \rightarrow R^3$ for a number of different values of wind speed module **u**, wind direction (or horizontal incidence angle) θ and vertical angle of incidence γ giving rise to $N_u \times N_\theta \times N_\gamma = 10 \times 40 \times 10 = 4000$ calibration points. From these number of experimental relations between the real and measured wind speed vector $\{u,v,w\}$ (or equivalent vector magnitude $\{|\mathbf{u}|,\theta,\gamma\}$) a proper fit of function $\mathbf{f}_c$: $R^3 \rightarrow R^3$ must be determined to be applied to correct future measurements.

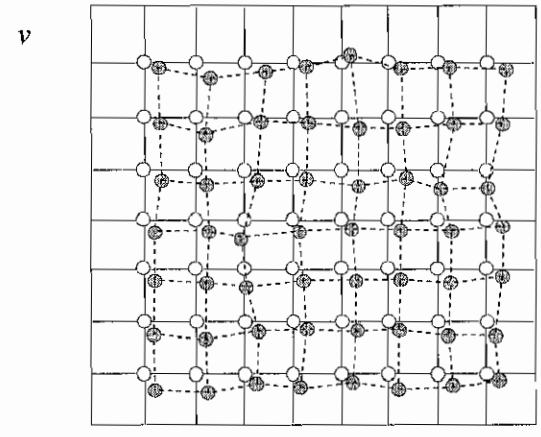

Fig. 10. Fig 6. Scheme of a two dimensional calibration results. The graphic relation $\mathbf{f}_c$: $R^2 \rightarrow R^2$ is presented. The white dots represent the wind tunnel measurements (real values of *u* and *v*), whereas the gray dots represent the

values measured by the sonic (measured values of *u* and *v*).

The authors have explored linear interpolation methods to reduce the information contained in the calibration test. The philosophy behind these method can be more easily illustrated if a two dimensional calibration is considered. If only a variation of two components of the wind speed *u* and *v* are evaluated (i.e. the two horizontal components) the relation between the measured and real values is represented graphically in Figure 9 where the white dots represent the calibration values for the vector $\{u,v\}$ and the gray dots the corresponding measured values $\{u^M,v^M\}$ (a similar scheme with a different data process is presented in [43]).

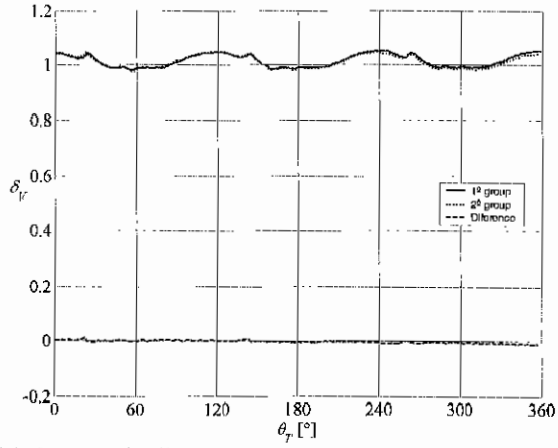

Fig 12. Fig 7. Ratio of the measured wind speed module on the real one (represented as δ_V) versus the incidence angle θ_T, obtained in two different tests (group 1 and 2). It is also represented the difference between both ratios.

The repeatability of the calibration results can be improved if the quality of the experimental set-up in wind tunnel is cared. In Figure 12 the results for the ratio between measured and real wind speed module δ_V for two different test in the same conditions and considering the MEASNET criteria for test quality are shown. The results shown that a large degree of repeatability is achieved.

3. References

[1] T.F. Pedersen, J-Å. Dahlberg, A. Cuerva, P. Eecen, P. Busche, A. Sanz-Andrés, F. Mouzakis, S. Franchini, Evaluation and Classification of Cup and Sonic Anemometry, EWEC 2006, Athens, 2006.

[2] Pardjack, E., Cuerva, A., Sonic Anemometry in Handbook of Experimental Fluid Mechanics. Springer-Verlag, Berlin 2007.

[28] J.C. Kaimal, J. Wyngaard, and D.A. Haugen, Deriving Power Spectra from a Three-Component Sonic Anemometer. Journal of Applied Meteorology, vol. 7, pp. 827-837, 1968.

[17] A. Grelle and A. Lindroth, Flow Distortion by a Solent Sonic Anemometer: Wind Tunnel Calibration and its Assessment for Flux Measurement over Forest Field Journal of Atmospheric and Oceanic Technology, vol. 11, pp. 1529-1542, 1994.

[15] C.A. Friehe, Effects of Sound Speed Fluctuations on Sound Anemometer Measurements. Journal of Applied Meteorology, vol. 15, pp. 607-610, 1976.

[41] J. Wyngaard, Transducer-Shadow Effects on Turbulence Spectra Measured by Sonic Anemometers Journal of Atmospheric and Oceanic Technology, vol. 2, pp. 548-558, 1985.

[1] Sonic Anemometers/thermometers-Part 1: Part 1 Acceptance Test Methods for Mean Wind Measurements ed. ISO. ISO/TC 146/SC 5/WG 2, 1997.

[2] European Wind Turbine Standards II eds. A. Dekker and J. Pierik. JOR3-CT95-0064, 1998. ECN. Petten.

[38] VDI, Turbulence Measurement with Sonic Anemometers ed. VDI. VDI 3786 Part 12, 1994. VDI.

[43] C. Kraan and W.A. Oost. A New Way of Anemometer Calibration and Its Application to a Sonic Anemometer. Journal of Atmospheric and Oceanic Technology: Vol. 6, No. 3, pp. 516–524.